


Article

Study of the Pore Water Pressure Development Characteristics of PHC Pipe Piles in Soft Soil Foundations

Zhaolin Jia ^{1,2,3,*}, Han Wu ^{1,2} , Shuaiqi He ^{1,2}, Qixiang Zhao ^{1,2} and Xiaoxu Zhang ^{1,2}

¹ School of Water Conservancy and Hydroelectric Power, Hebei University of Engineering, Handan 056038, China; wuhan990317@163.com (H.W.); heshuaiqi477@163.com (S.H.); 15544778856@163.com (Q.Z.); zxx1844525319@163.com (X.Z.)

² Hebei Key Laboratory of Intelligent Water Conservancy, Hebei University of Engineering, Handan 056038, China

³ State Key Laboratory of Geomechanics and Geotechnical Engineering, Institute of Rock and Soil Mechanics, Chinese Academy of Sciences, Wuhan 430071, China

* Correspondence: jiazhaolin@zohomail.cn

Abstract: When constructing hollow prestressed high-strength concrete (PHC) pipe piles in soft soil foundations, the generation and dissipation of pore water pressure can induce negative friction on the pile. This phenomenon increases the settlement of the pile foundation and, in severe cases, can lead to pile deflection and flotation. To further investigate the development characteristics of pore water pressure during PHC hollow pipe pile driving in soft soil, this study combined existing theories and numerical models to analyze the generation and influence areas of pore water pressure. Field tests were conducted at three different sites: an untreated site, a surcharge preloading site, and a site treated with cement mixing piles and well dewatering. These tests monitored and analyzed the horizontal and vertical development and behavior of pore water pressure during pile driving at each site. The results indicate that during the pile driving process, when the horizontal distance from the pile center is 3d and 9d, the peak values of the excess pore water pressure in the site treated with cement mixing piles and well dewatering are 117 kPa and 100 kPa. After pile driving is completed, they decrease to 50 kPa and 48 kPa, respectively. The peak values of excess pore water pressure in the surcharge preloading site are 122 kPa and 97 kPa, and after pile driving, they decreased to 80 kPa and 21 kPa, respectively. The peak values of excess pore water pressure in untreated sites are 140 kPa and 121 kPa; after pile driving, they decreased to 82 kPa and 60 kPa, respectively. Pore water pressure increases with the depth of pile driving and decreases with distance from the pile driving location. The peak pore water pressure and dissipation rate during construction were found to be higher at the untreated site compared to the other two sites. Therefore, during pile sinking in soft soil foundations, dewatering and driving drainage boards are effective methods for reducing pore water pressure and accelerating its dissipation. These findings provide a theoretical basis and technical support for ensuring the safety of engineering constructions.

Keywords: PHC pipe pile; excess pore water pressure; field test; pore pressure monitoring



Citation: Jia, Z.; Wu, H.; He, S.; Zhao, Q.; Zhang, X. Study of the Pore Water Pressure Development Characteristics of PHC Pipe Piles in Soft Soil Foundations. *Buildings* **2024**, *14*, 1976. <https://doi.org/10.3390/buildings14071976>

Academic Editor: Harry Far

Received: 24 May 2024

Revised: 19 June 2024

Accepted: 25 June 2024

Published: 30 June 2024



Copyright: © 2024 by the authors. Licensee MDPI, Basel, Switzerland. This article is an open access article distributed under the terms and conditions of the Creative Commons Attribution (CC BY) license (<https://creativecommons.org/licenses/by/4.0/>).

1. Introduction

Pile foundations are extensively utilized in geotechnical engineering, hydraulic engineering, and other professional fields due to their strength, stability, and other advantageous properties. Hollow prestressed high-strength concrete (PHC) pipe piles are particularly prominent among various types of piles because of their high concrete strength, excellent penetration capabilities, and the convenience and speed of their construction [1–4]. However, the application of PHC hollow pipe piles is subject to certain limitations due to their inherent characteristics. Specifically, their performance in saturated soft soil conditions is suboptimal, which restricts their scope of application and usage conditions. The use of PHC hollow pipe piles in saturated soft soil foundations can lead to several issues:

(1) During pile driving, the soil squeezing effect may occur, causing ground uplift, pile upwelling, displacement, and even fractures. (2) After the construction of the pile foundation, it is possible that due to the dissipation of pore water pressure in saturated soft soil, the soil layer may experience reconsolidation settlement, resulting in the negative frictional resistance of the pile, reducing the bearing capacity of the pile foundation, and increasing the settlement of the pile foundation. (3) The horizontal seismic resistance of the pile is low. (4) During excavation, the unloading effect of the soil can cause stratum movement, resulting in soil uplift at the bottom of the foundation pit, causing the piles at the bottom to float and deflect. In severe cases, this can lead to problems such as the inclination and fracture of pile groups [5,6]. Analyses of pore water pressure in soils have been investigated via both deterministic and stochastic analyses, as well as machine learning applications [7,8].

In practical engineering, various calculation methods have been proposed to understand the influence of excess pore water pressure [9–12]. Numerous domestic and international scholars have conducted research on the excess pore water pressure generated during pile driving, analyzing its dissipation and variation patterns and proposing methods to mitigate its impact. Dhanya Dhanya Ganesalingam et al. [13] utilized Plaxis software to study the influence of different pore water pressure distribution modes on the consolidation behavior of cylindrical soil layers. Mohammadreza Khanmohammadi and Kazem Fakharian [14] investigated the dissipation of pore water pressure in saturated clay and the soil consolidation process using finite element software. Yonghong Wang et al. [15] employed silicon piezoresistive sensors to measure the excess pore water pressure of PHC pipe piles during pile driving through field tests, analyzing the change law of excess pore water pressure at the pile–soil interface. Jianwen Ding et al. [16] explored the correlation between structural changes in marine soft soil and the generation and dissipation of excess pore water pressure in practical engineering contexts. Pengpeng Ni et al. [17] concluded through model tests that permeable piles can accelerate the dissipation of pore pressure and soil consolidation, with this improvement being more effective in group piles. Yansong Yang et al. [18] analyzed the influence of the cone hole’s layout, hole diameter, radial distance, and pile depth on the variations in excess pore water pressure using laboratory model experiments, finding that cone perforated pipe piles can expedite the dissipation of excess pore water pressure. Hu Xiangqian et al. [19,20] proposed control parameters for precast pile construction by studying the excess pore water pressure caused by piling after the installation of drainage boards in saturated soft clay on site. Mohammed Y. Fattah and Faris S. Mustafa [21] conducted a model experiment to study the effects of factors such as the slenderness ratio of the pile, the operating frequency of the machines, and the soil permeability on the excess pore water pressure generated in saturated sandy soil. Mohammed Y. Fattah et al. [22] used the finite element method to analyze the pile–soil model under undrained conditions, solved the stress problem of the pile–soil system under undrained conditions, and revealed the influence of pore water pressure on soil stiffness and strength. From the above, it is evident that there is relatively limited research on engineering measures that reduce the pore water pressure generated by driving hollow PHC pipe piles into soft soil foundations at the current stage.

In this paper, to further investigate the generation and dissipation of excess pore water pressure during the construction of PHC hollow pipe piles in soft soil foundations, a theoretical analysis was conducted, followed by on-site in situ tests at three selected locations: an untreated site, a surcharge preloading site, and a site treated with cement mixing piles and well dewatering. The distribution and dissipation patterns of excess pore water pressure caused by the construction of pile foundations in saturated soft clay, following the installation of plastic drainage plates, dewatering wells, and surcharge, were analyzed. Additionally, the factors affecting engineering outcomes were discussed. Based on engineering practice, a safety control method for constructing PHC hollow pipe piles in saturated muddy clay is proposed, offering valuable conclusions that can be referenced in similar projects.

2. Theoretical Analysis

When the pile foundation is driven, its inherent volume exerts a squeezing force on the surrounding soil, causing it to spread radially outward and resulting in soil displacement [23]. In the shallow soil layers with low overburden pressure, this displacement leads to upward bulging, loosening the upper soil mass. Consequently, this part of the pile shaft experiences low friction and relatively small excess pore water pressure. However, as the depth increases, the overburden pressure rises, limiting soil displacement. This increases the friction on the pile shaft at these depths and correspondingly raises excess pore water pressure [24]. Upon driving the pile foundation into the soil, the surrounding soil mass is compressed, exerting pressure on the groundwater. This pressure exceeds the original hydrostatic pressure, creating excess pore water pressure [25–27].

Excess pore water pressure influences soils with various properties [28–30]. During pile driving with a pile hammer, due to the length of the seepage path and soil permeability, the excess pore water pressure generated cannot fully dissipate between hammer blows. Instead, it accumulates progressively as pile driving continues. This accumulation and subsequent dissipation of excess pore water pressure affect the effective stress between soil masses, thereby impacting the pile driving process and construction outcomes [31,32].

During pile driving, the soil around the pile is divided into four zones, A, B, C, and D, as depicted in Figure 1 [33]. Zones A and B are the closest to the pile; hence, the excess pore water pressure generated in these areas is significantly higher than in zones C and D, indicating a more pronounced impact of pile driving on the soil. While zone C is affected to a certain extent, the impact is considerably less than in zones A and B, with the pore water pressure generated in zone C being minimal to negligible. Zone D remains unaffected, representing the undisturbed soil area on site.

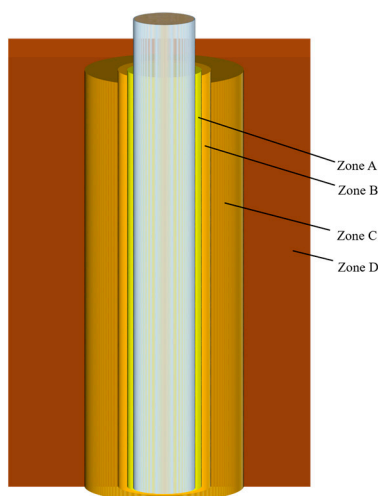


Figure 1. Zones formed around the pile after pile driving.

When a pile with a radius of R_1 sinks into infinite soil, a stress influence zone will be formed around the pile, as shown in Figure 2. The circular area surrounding the small hole will transition from an elastic state to a plastic state. As the pressure inside the small hole continues to increase, the plastic zone continues to expand until the internal pressure increases to the ultimate pressure P_u . The radius at the junction of elasticity and plasticity is R , and the soil remains in an elastic state beyond the radius R . Under the premise of axial symmetry, all points on a concentric circular surface have the same stress state, so the radial stress σ_r , tangential stress σ_θ , and longitudinal stress σ_z of the small hole are all principal stresses, as shown in Figure 3 [24,34].

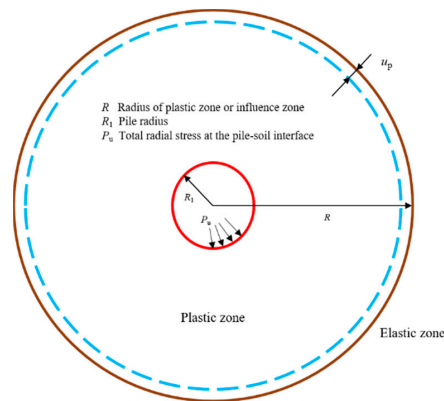


Figure 2. Cylindrical small-hole expansion model.

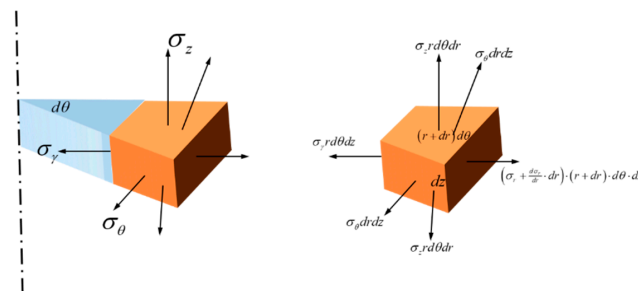


Figure 3. Axisymmetric cylindrical expansion model.

Based on the equilibrium conditions of the radial force system, Formulas (1)–(3) can be derived:

$$\left(\sigma_r + \frac{d\sigma_r}{dr} \cdot dr\right) \cdot (r + dr) \cdot d\theta \cdot dz - \sigma_r r d\theta \cdot dz - \sigma_\theta dr \cdot d\theta \cdot dz = 0 \tag{1}$$

$$\frac{d\sigma_r}{dr} + \frac{\sigma_r - \sigma_\theta}{r} = 0 \tag{2}$$

$$\sigma_r - \sigma_\theta = (\sigma_r + \sigma_\theta) \sin \varphi + 2c \cdot \cos \varphi \tag{3}$$

where r is the distance from the center of the hole to any point; and c and φ , respectively, represent the cohesive force and friction angle of the soil. The boundary conditions for displacement and stress in the plastic zone are shown in Formulas (4) and (5)

$$r = R_i, \sigma_r = P_u \tag{4}$$

$$\sigma_r - \sigma_\theta = 2c_u \tag{5}$$

Among them is undrained strength. By considering the solution of the plane strain-state differential equation, the total stress increment in any radial and tangential directions of the plastic zone can be calculated using Formulas (6) and (7):

$$\frac{\sigma_r}{c_u} = 2 \ln \frac{R_i}{r} + \frac{P_u}{c_u} \tag{6}$$

$$\frac{\sigma_\theta}{c_u} = 2 \ln \frac{R_i}{r} + \frac{P_u - 2c_u}{c_u} \tag{7}$$

In order to obtain the radius R of the plastic zone, the displacement at the boundary of the plastic zone is described in Formula (8):

$$\mu_p = \frac{1 + \mu}{E} R c_u \tag{8}$$

Assuming that the soil in the plastic zone is incompressible, Formula (9) is obtained:

$$\pi R_i^2 = \pi R^2 - \pi(R - u_p)^2 \quad (9)$$

The above equation is substituted and high-order trace elements are omitted to obtain Formula (10):

$$\frac{R}{R_i} = \sqrt{\frac{E}{2(1 + \mu)c_u}} \quad (10)$$

The pressure on the pile–soil interface can be obtained from the front, which is called the small hole expansion pressure P_u , as shown in Formula (11):

$$\frac{P_u}{c_u} = \ln \frac{E}{2(1 + \mu)c_u} + 1 \quad (11)$$

Among them, μ is the Poisson's ratio of soil, and under undrained conditions, μ can be taken as 0.5.

Due to the "soil plug effect" of prestressed concrete hollow piles [4,35], when determining the ratio of plastic zone radius to expansion hole radius R/R_i , the initial radius R_i of the small hole can be taken as the mean of the outer radius R_1 and inner radius R_2 of the prestressed concrete hollow pile: that is, $R_i = (R_1 + R_2)/2$. The calculation method is shown in Formula (12):

$$\frac{R}{R_i} = \sqrt{\frac{E}{2(1 + \mu)c_u}} \quad (12)$$

Based on the characteristics of soft soil, the Mohr–Coulomb elastoplastic constitutive model was adopted. The active–passive contact algorithm in ABAQUS was utilized for interactions between the pile body and soil. The high-stiffness surface of the pile body was designated as the active surface, while the soil surface is the passive surface [36]. The sliding friction coefficient μ at the interface was set to 0.2. The pile body followed an elastic constitutive model. The soil dimensions were 20 m in height and 15 m in width. The pile length was set to 13 m (representing one section of the pile length in actual engineering), with the pile penetrated 12 m into the mud. The element type selection for the pile is CPE4R. The element type selection for the soil is CPE4P. The model grid division diagram is shown in Figure 4.

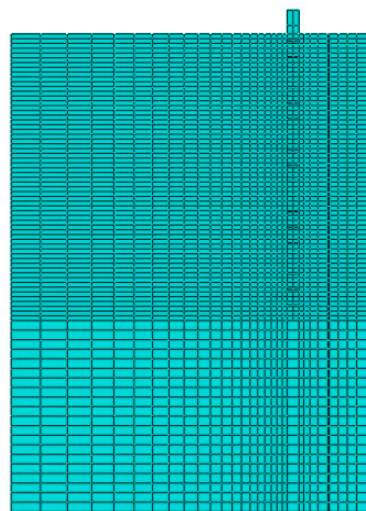


Figure 4. Model grid division.

At a distance of 2.4 m from the pile, a linearly increasing excess pore water pressure was applied along the length of the pile. The excess pore water pressure was 0 at the top

of the pile and reached 552 kPa at the bottom. This value was calculated as the sum of 4.6 times the static water pressure and 2.56 times the self-weight pressure of the overlying soil. The numerical calculation model and pore water pressure settings are shown in Figures 5 and 6.



Figure 5. Numerical calculation model.

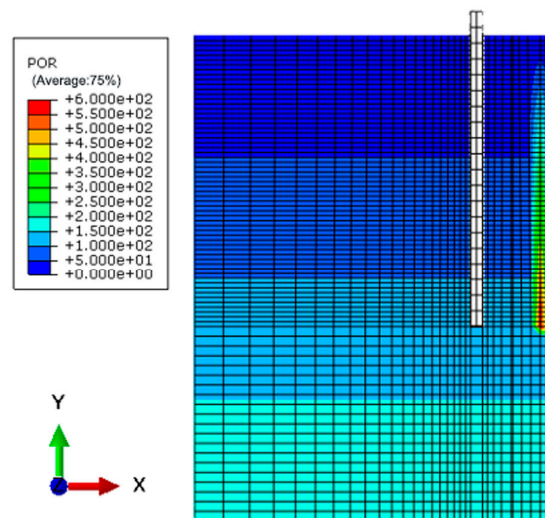


Figure 6. Pore water pressure setting.

The numerical calculation results are shown in Figure 7. The driven pile creates a distribution of unbalanced excess pore water pressure in the surrounding soil. In soft clay, if the pore water pressure is not dissipated promptly, seepage will occur toward areas of lower pore water pressure potential. This seepage alters the initially unbalanced distribution of pore water pressure, which in turn changes the distribution of total stress in the soil and subsequently the distribution of effective stress. Therefore, the excessive pore water pressure generated by pile driving can modify the seepage field, leading to changes in the stress field within the soil and causing the displacement of both the soil and the piles.

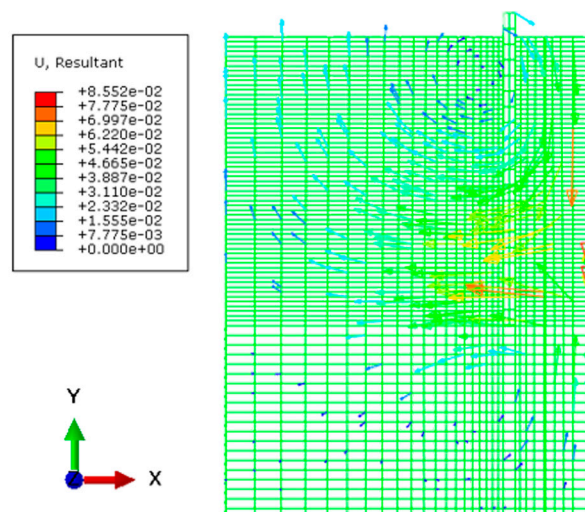


Figure 7. Numerical model calculation result.

3. Test Site and Test Content

3.1. Overview of Test Site

The research project site is located in Tianjin; it is situated on the North China Plain and is characterized by alluvial and marine low plains. Following vacuum preloading treatment, the site was filled with approximately 1.00 m of plain fill. The terrain of the site varies, with elevations ranging between 4.11 m and 3.22 m. According to survey data, the foundation soil within a depth of 35.00 m is divided into nine layers based on mechanical properties. The physical and mechanical indices of each foundation soil layer are detailed in Table 1.

Table 1. Physical and mechanical properties of soil layers.

Soil Type	Soil Thickness (m)	Moisture Content ω (%)	Severe γ (kN/m ³)	Void Ratio e	Liquidity Index I_L	Compressibility Coefficient a_{1-2} (1/Mpa)	Compression Modulus E_s (Mpa)
Plain fill	1.5~3	28.4	19.4	0.82	0.78	0.49	3.47
Dredger fill	2.8~6.6	47.49	17.39	1.34	1.02	0.89	2.63
Clay	9.5~12.8	41.67	17.87	1.18	0.82	0.72	3
Silty clay	2~2.4	28.2	19.3	0.82	0.75	0.35	5
Silty clay	1.7~2	25.96	19.67	0.73	0.72	0.34	5.15
Silty clay	1.8~3.3	24.16	20.13	0.66	0.57	0.29	5.65
Silt	1.2~2.2	23.2	20.08	0.65		0.13	12.01
Silty clay	5.2~9	23.8	20.1	0.66	0.46	0.29	5.84
Silty sand	4.10	27.49	19.13	0.79		0.16	10.93

For this test, three sites were selected as test points based on different foundation treatment schemes: an untreated site, a surcharge preloading site, and a site treated with cement mixing piles and well dewatering. The untreated site consists of the original soil without any treatment, where PHC hollow pipe piles are driven directly, serving as a baseline for comparing test results.

According to the design, the surcharge preloading site requires preloading loads (such as soil and stones) to be stacked on the construction site one month in advance. Additionally, a drainage board is placed 0.2 m away from each pile position along the central line of two adjacent pile positions and its extension line. Another drainage board is set at the midpoint of the central line of adjacent pile positions. The remaining vacant positions on the site are filled with drainage boards spaced 1 to 1.2 m apart on the board surface or 0.8 to 1 m apart at the board tip. The drainage boards are arranged in a rectangular pattern [37],

with a driving depth of 0.5 to 1.0 m through the soft soil layer. The layout of the surcharge preloading site is illustrated in Figure 8.

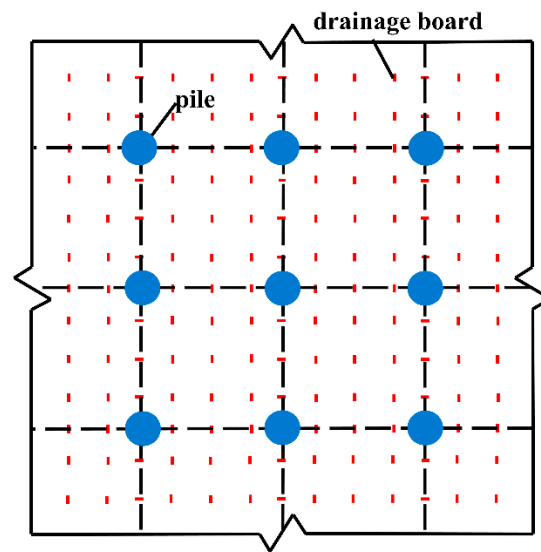


Figure 8. Layout of surcharge preloading site.

According to the design for the cement mixing pile and well dewatering site, dewatering wells are drilled at the edges of the pile location area, with one dewatering well for every 300 to 400 square meters. Each dewatering well has a diameter of 0.5 m and a depth ranging from 12 to 20 m. These wells are used to lower the groundwater level by 5 to 6 m. The PHC hollow pipe piles are arranged in a square pattern on the test site, with a center-center distance of 2.5 m between adjacent piles. The cement mixing pile holes are arranged in a rectangular pattern and positioned at the midpoint of the central line of the PHC hollow pipe piles. The cement mixing piles have a diameter of 0.5 m and a length of 6 m, and their tips penetrate 0.5 to 1 m through the soft soil layer. After constructing the cement mixing piles, dewatering continues for approximately 7 days to solidify the piles. The layout of the cement mixing pile and well dewatering site is illustrated in Figure 9.

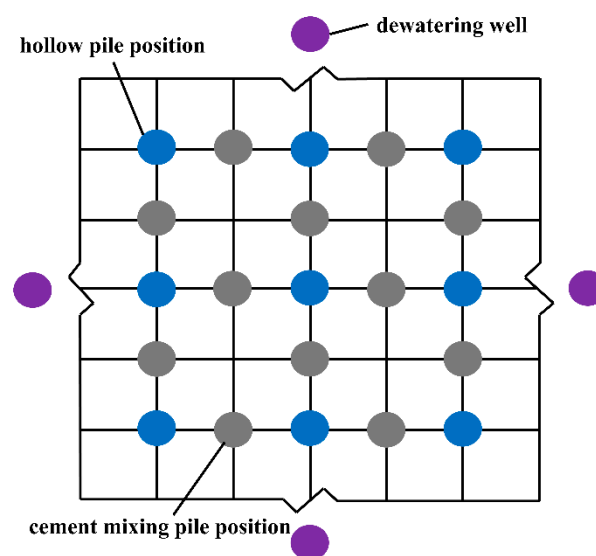


Figure 9. Layout of cement mixing pile and well dewatering site.

3.2. TGCY-1-100 Pore Water Pressure Gauge

The TGCY-1-100 pore water pressure gauge selected for this test is a vibrating wire sensor. This sensor can monitor not only pore water pressure or liquid levels but also the temperature at the measurement point. The corresponding engineering tester, shown in Figure 10, can be used for automatic measurement or dynamic monitoring.



Figure 10. Multi-channel signal acquisition instrument.

The working principle of the vibrating wire pore water pressure gauge is based on the deformation of the pressure-bearing membrane under applied pressure. This deformation alters the tension of a steel wire fixed to the membrane, thereby changing its natural vibration frequency. A frequency gauge detects this natural vibration frequency, allowing the relationship between the vibration frequency and the applied pressure (pore water pressure) to be expressed by Formulas (13)–(15) [38]:

$$P = k(F_i - F_0) \quad (13)$$

$$F_i = f_i \times 10^{-3} \text{ Hz}^2 \quad (14)$$

$$F_0 = f_0 \times 10^{-3} \text{ Hz}^2 \quad (15)$$

where P is the pore's water pressure, measured in kPa; and k is the sensor coefficient, which is related to the size and material properties of the pressure-bearing membrane and steel string. The value of 10^{-4} kPa/Hz² is determined through indoor calibration and is expressed in kpa/10³ Hz². F_0 is the initial modulus, F_i is the current modulus, f_i is the current frequency, and f_0 is the initial frequency, all measured in Hz.

The pore water pressure (kPa) at any given time can be determined by measuring the natural frequencies of the steel string at different points. Factors such as air temperature, atmospheric pressure, and altitude significantly affect the measured values of the pore water pressure gauge. Therefore, the reference value for the pore water pressure gauge is obtained when the measured value stabilizes in the field environment without bearing water pressure. When the pore water pressure gauge is placed in a water-free location in the borehole (typically for 0.5 h), a reading meter is used to measure and record the value. After the value stabilizes, two consecutive measurements are taken, and their average is used as the reference value.

For determining the range of pore water pressure, it is necessary to estimate the static and dynamic pore water pressures. For example, when the burial depth is 10 m, the estimated range of the pore water pressure gauge is as follows [39,40].

Assuming that the groundwater level is 1.5 m below the surface, the calculation method for pore water pressure is shown in Formula (16):

$$P_w = K\gamma_w H = (1 - \sin \phi)\gamma_w H = 85 \text{ kPa} \quad (16)$$

For the calculation of dynamic water pressure, assuming complete soil liquefaction, when the excess pore water pressure reaches the confining pressure or the weight of the overlying soil, the calculation method for excess pore water pressure is shown in Formula (17):

$$P_s = K_0 \gamma H = (1 - \sin \phi') \gamma H = 185 \text{ kPa} \quad (17)$$

In the formula, the maximum value K_0 is taken as 1. According to existing exploration data, the value of γ is between 17 and 19 kN/m³. According to the above formula, when the soil liquefies, excess pore water pressure reaches the surrounding soil, confining pressure. At this time, the sum of static water pressure and dynamic water pressure will not exceed 270 kPa. To ensure the accuracy requirements of the pore water pressure gauge, the selected range should not be too large. The upper limit value of the pore pressure gauge should be greater than the sum of the static water pressure value and the estimated excess pore water pressure value by 150 kPa.

3.3. Test Contents

3.3.1. Burying and Installation of Pore Water Pressure Gauge

In this test, suitable locations at horizontal distances of 3d and 9d from the center of the pile to be driven were selected as measuring points at each site, as illustrated in Figure 11. Two test depths were chosen for each measuring point, with pore water pressure gauges buried at depths of 4 m and 10 m. Each site included two groups of tests, resulting in four sets of collected data.

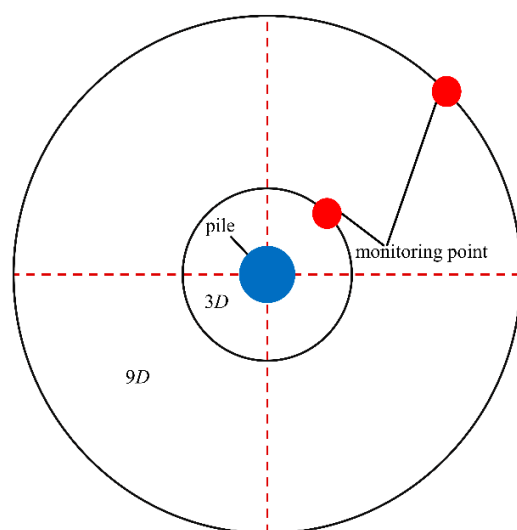


Figure 11. Layout of monitoring points for pore water pressure gauge.

The pore water pressure gauge's installation requires drilling a vertical hole with a diameter of 200 mm. In the filling layer or other loose and unstable shallow soil layers, casings should be used for hole protection. During the test, it is ensured that the casing is vertical and free of sediment or thick slurry. The hole's inclination must be strictly controlled, with the instrument suspended and straightened using fine lead wires to accurately measure the depth and ensure the precise elevation of the buried pore water pressure gauge. Before installing the pore water pressure gauge, the permeable stone is removed and soaked at its tip in water for over 24 h to eliminate air. The cavity at the tip of the gauge is filled with clean water, and the permeable stone is installed while submerged in clean water. The entire instrument should be immersed in clean water before burial. To ensure that the water inlet of the gauge remains unblocked and to prevent cement slurry blockage, the instrument is cleaned with water and wrapped in saturated medium and fine sand during burial. In this test, to ensure that the pore water pressure gauge is lowered vertically and the water inlet remains unblocked, a small plastic basket with a diameter of

25 cm and a height of 30 cm, and of sufficient strength, is used. A cylindrical bag made of geotextiles, with an open bottom, is filled with wet coarse sand. The pore water pressure gauge is inserted into the bag, and the bag is placed in the plastic basket, as shown in Figure 12. A nylon rope of corresponding length was used to lift the basket vertically to the specified elevation. During burial, it is crucial to prevent the outflow of water pre-injected into the gauge cavity to maintain the reliability of measurements.



Figure 12. Installation of pore water pressure gauge.

3.3.2. Test Arrangement and Monitoring Content

Exploratory holes for measuring the groundwater level should be drilled 3–5 days before the pile driving test. Backfill materials consisting of coarse sand and clay balls were prepared, with a total of 0.68 m³ of coarse sand and 2.3 m³ of clay. The clay balls should have a diameter of approximately 2 cm and exhibit a certain grading. The prepared clay balls are air-dried in a cool place, avoiding direct sunlight or artificial heating. On the day before the test, the hole was drilled at the measuring point, and the pore water pressure gauge was installed. Prior to pile driving, the groundwater level and the initial hydrostatic pressure for each pore pressure gauge were measured. The test pile was driven, and changes in pore water pressure were monitored during pile driving until the pore water pressure stabilized. This process will yield a complete model of pore water pressure growth and dissipation.

Monitoring focuses on the growth and dissipation laws of pore water pressure during continuous hammering, the distribution of excess pore water pressure along both the pile shaft direction and the horizontal direction, and the growth and changes in pore pressure during single pile driving.

4. Test Results and Analysis

Through the monitoring of three test sites, namely, the cement mixing pile and well dewatering site, the surcharge preloading site, and the untreated site, the study analyzes the distribution and dissipation patterns of excess soil pore water pressure caused by the construction of a single pile in saturated soft clay. This is carried out after the installation of plastic drainage plates, dewatering wells, and surcharges. Additionally, the relationship between excess pore water pressure and the effective self-weight of the overlying soil is examined, and the factors affecting the engineering outcomes are identified.

The variation in pore water pressure at the cement mixing pile and well dewatering site is shown in Figure 13.

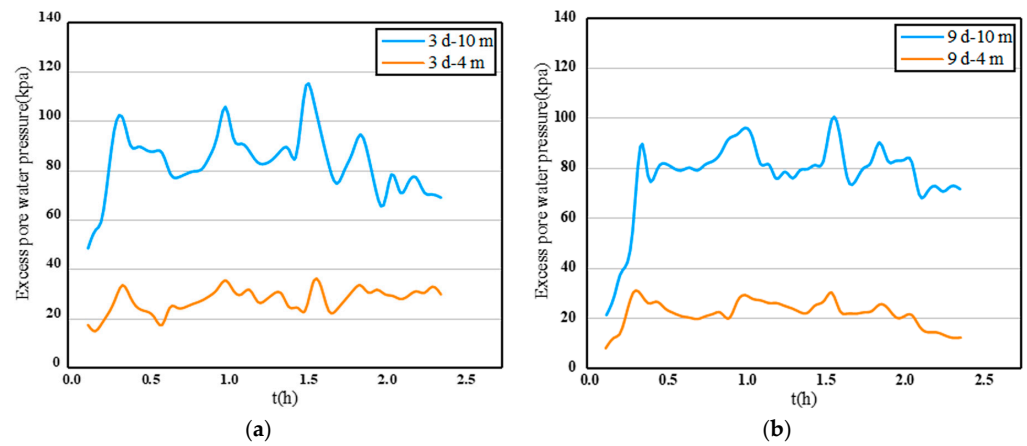


Figure 13. Variation in excess static pore water pressure at the cement mixing pile and well dewatering site: (a) 3d from the pile center; (b) 9d from the pile center.

The variation in the pore water pressure of the surcharge preloading site is shown in Figure 14.

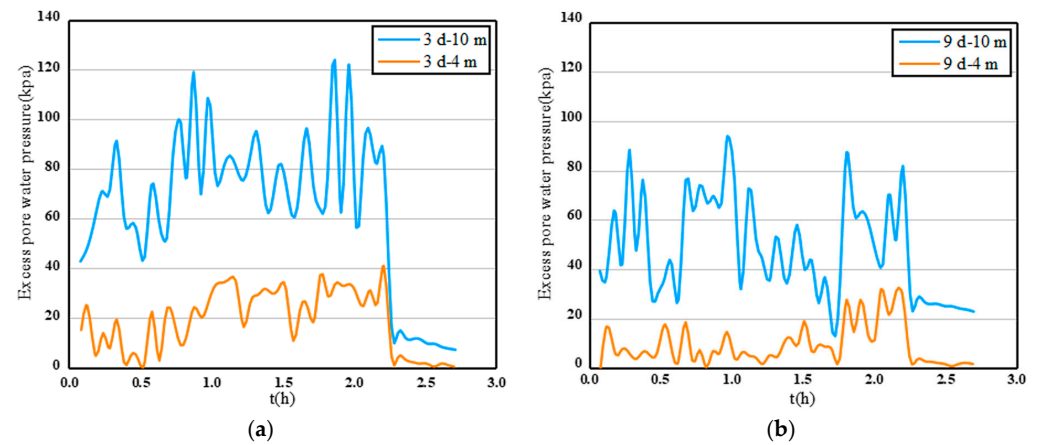


Figure 14. Variation in excess static pore water pressure at the surcharge preloading site: (a) 3d from the pile center; (b) 9d from the pile center.

The variation in the pore water pressure of the untreated site is shown in Figure 15.

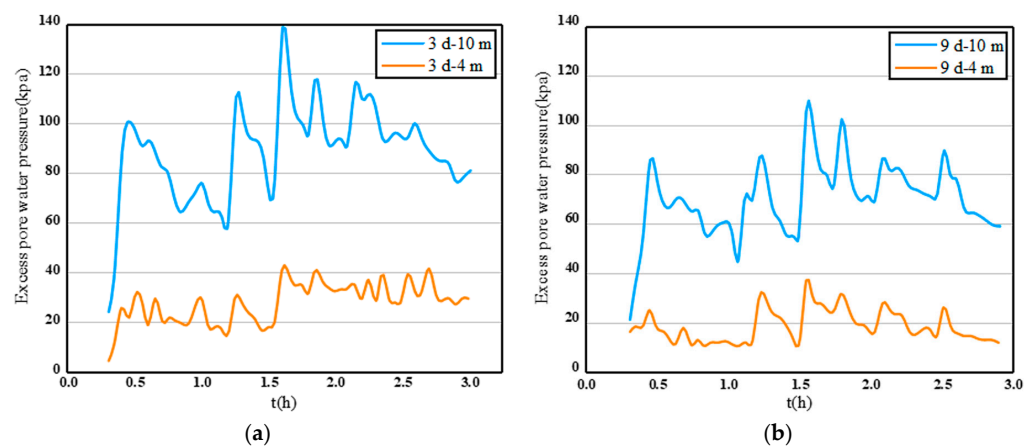


Figure 15. Variation in excess static pore water pressure at the untreated site: (a) 3d from the pile center; (b) 9d from the pile center.

From the above figure, it can be observed that the distribution of excess pore water pressure increases with depth and decreases with the horizontal distance from the pile center, ranging from 3d to 9d.

From the above figure, it can be observed that the excess pore water pressure dissipates rapidly during the intervals between pile driving. However, during one and the next hammering processes, the generated pore water pressure will not completely dissipate, and the remaining excess pore water pressure will continue to accumulate during the pile driving process. At the cement mixing pile and well dewatering site, the excess pore water pressure at a distance of 3d decreases from a maximum of 117 kPa to 50 kPa, and at a distance of 9d, it decreases from 100 kPa to 48 kPa. At the surcharge preloading site, the excess pore water pressure at a distance of 3d decreases from a maximum of 122 kPa to 80 kPa, and at a distance of 9d, it decreases from 97 kPa to 21 kPa. At the untreated site, the excess pore water pressure at a distance of 3d decreases from a maximum of 140 kPa to 82 kPa, and at a distance of 9d, it decreases from 121 kPa to 60 kPa.

When the depth is 10 m, the ratio of excess pore water pressure at different horizontal distances at the same depth is 1.17, 1.25, and 1.15 for the cement mixing pile and well dewatering site, the surcharge preloading site, and the untreated site, respectively. At 4m, it is 1.6, 1.56, and 1.21, respectively. When the horizontal distance is 3 m, the ratio of excess pore water pressure at different depths at the same horizontal distance is 2.92, 2.44, and 2.75 for the cement mixing pile and well dewatering site, the surcharge preloading site, and the untreated site, respectively. When the horizontal distance is 9 m, it is 4.0, 3.03, and 2.9, respectively. These ratios indicate that depth significantly impacts excess pore water pressure. However, adjusting the pile spacing can also effectively control the influence of excess pore water pressure.

The relationship between the excess pore water pressure and the effective overburden pressure of the soil mass during the driving of PHC hollow pipe piles is illustrated in Figures 16–18. Specifically, Figure 16 shows this relationship for the cement mixing pile and well dewatering site.

The relationship between excess pore water pressure and the effective overburden pressure of the soil mass at the surcharge preloading site is shown in Figure 17.

The relationship between excess pore water pressure and the effective overburden pressure of the soil mass at the untreated site is shown in Figure 18.

The ratio of excess pore water pressure to effective overburden pressure caused by a single pile is influenced by the depth of the soil layer, the distance between pile centers, and soil properties. This ratio increases with depth and decreases with increasing horizontal distance from the pile center.

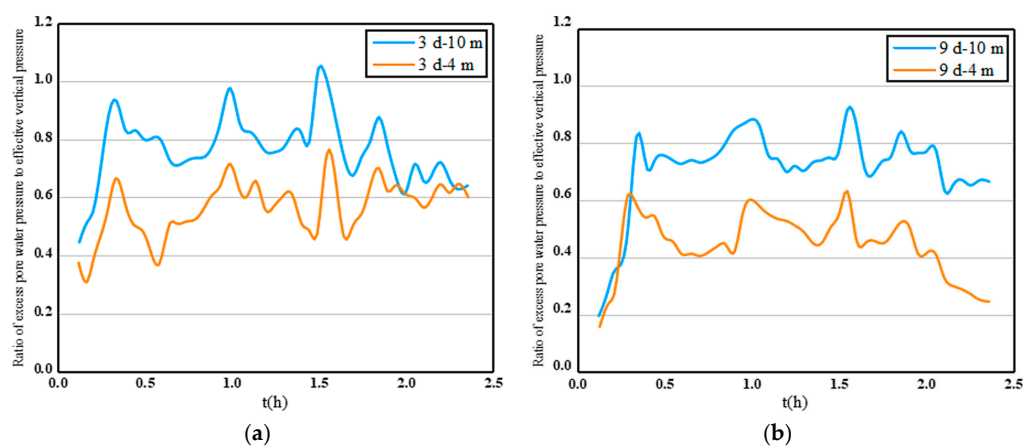


Figure 16. Relation between excess pore water pressure and the effective overburden pressure of the soil mass at the cement mixing pile and well dewatering site: (a) 3d from the pile center; (b) 9d from the pile center.

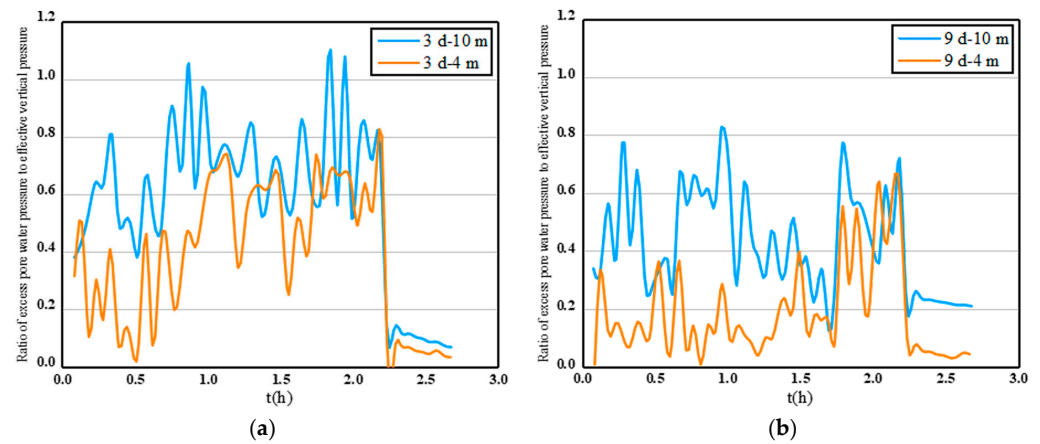


Figure 17. Relation between the excess pore water pressure and the effective overburden pressure of the soil mass at the surcharge preloading site: (a) 3d from the pile center; (b) 9d from the pile center.

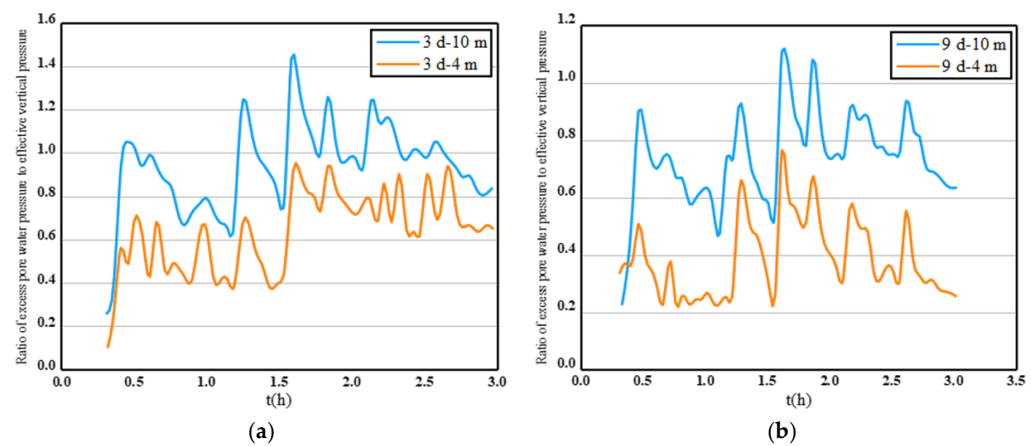


Figure 18. Relation between the excess pore water pressure and the effective overburden pressure of the soil mass at the untreated site: (a) 3d from the pile center; (b) 9d from the pile center.

Comparing the ratio of excess pore water pressure to the effective self-weight of overburdened soil at each measuring point 3d from the pile center, the peak value at the untreated site during pile driving is 1.44. This is higher than the values at the cement mixing pile and well dewatering site, as well as the surcharge preloading site, indicating an overall higher level at the untreated site. This suggests that both the installation of cement mixing and dewatering wells and the use of drainage boards can effectively reduce the excess pore water pressure generated during pile driving.

Subsequent pile driving has a noticeable superposition effect on the pore water pressure at the site. The distribution of excess pore water pressure across the three sections is largely consistent, with preloading, cement mixing piles, and well dewatering measures enhancing the dissipation rate of pore water pressure, as shown in Figure 19. The initial groundwater level at the cement mixing pile and well dewatering site is 3 m lower than at the untreated site, and the excess pore water pressure caused by temporary issues during pile driving does not diminish the corresponding value. Overall, implementing dewatering wells, drainage boards, and other drainage measures can significantly reduce the excess pore water pressure generated during pile driving and accelerate its dissipation process.

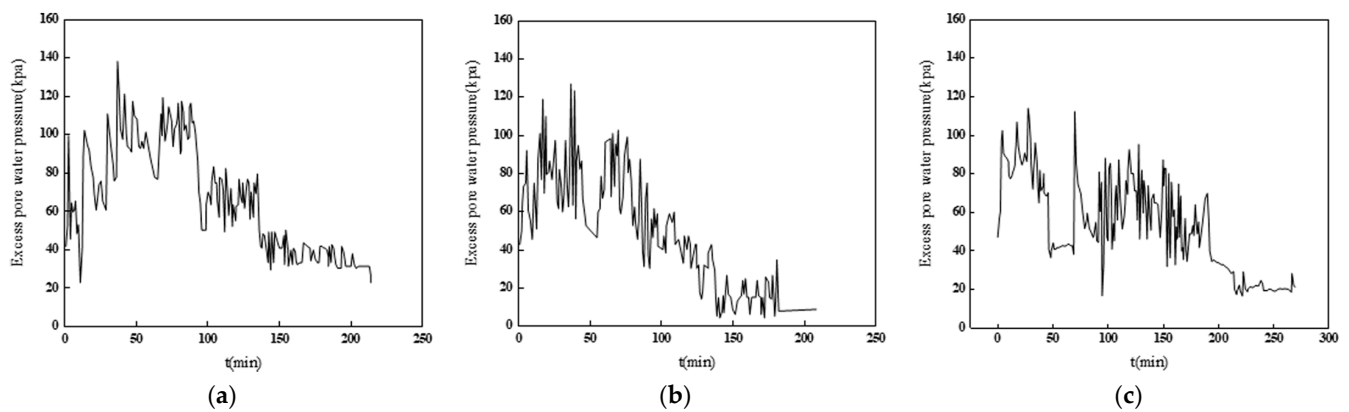


Figure 19. Whole process of pore water pressure growth and dissipation at the three test sites: (a) change process of pore water pressure at the untreated site; (b) change process of pore water pressure at the surcharge preloading site; (c) change process of pore water pressure at the cement mixing pile and well dewatering site.

5. Conclusions

Through theoretical analysis and field tests, the development characteristics of excess pore water pressure generated during PHC hollow pipe pile driving in soft soil foundations were studied. Based on these findings, engineering measures are proposed to reduce the excess pore water pressure generated during the construction of PHC hollow pipe piles in soft soil foundations and to enhance their performance in such conditions.

Based on existing theoretical results, the influence and affected areas of excess pore water pressure generated during PHC hollow pipe pile driving are analyzed. To mitigate this influence in soft soil foundations, engineering measures such as site treatment with cement mixing piles, well dewatering, and surcharge preloading are proposed for PHC hollow pipe pile construction sites.

Through pore pressure monitoring tests at three sites—untreated, surcharge preloading, and cement mixing pile with well dewatering—the horizontal and vertical distribution patterns of excess pore pressure were obtained. The results demonstrate that the distribution of excess pore water pressure increases with depth from 4 m to 10 m and decreases with horizontal distance from 3d to 9d. The excess pore water pressure dissipates quickly during the interval of pile driving, but the excess pore water pressure generated by one pile driving is not enough to dissipate completely during the next pile driving. Therefore, excess pore water pressure will gradually accumulate. During the pile driving process, the maximum value of the excess pore water pressure was 140 kPa in the untreated site. At this time, the burial depth of the pore pressure gauge was 10 m, and the horizontal distance from the pile center was 3d. When the pile driving was completed, excess pore water pressure at this point dropped to 82 kPa. When the burial depth of the pore pressure gauge is 10 m and the horizontal distance from the pile center is 9d, the peak value of the excess pore water pressure during the pile driving process is the lowest at the surcharge preloading site, which was 97 kPa. After pile driving was completed, it dropped to 21 kPa.

When the burial depth of the pore pressure gauge is 10 m, the ratio of excess pore water pressure at different horizontal distances at the same depth was 1.17, 1.25, and 1.15, respectively, in three test sites: cement mixing pile and well dewatering site, surcharge preloading site, and untreated site. When the burial depth of the pore pressure gauge was 4 m, the ratio was 1.6, 1.56, and 1.21. The ratio of excess pore water pressure at different depths at the same horizontal distance is generally greater than that at different horizontal distances at the same depth. Therefore, it can be seen that depth has a greater impact on excess pore water pressure during pile driving compared to horizontal distance. However, reasonable control of spacing can also reduce the impact of excess pore water pressure during pile driving.

The distribution of excess pore water pressure corresponding to the three test sites is the same, and the subsequent pile driving process has a significant superposition effect on the pore water pressure of the three sites. Due to the nature of the soil, pile driving caused a significant peak in excess pore water pressure. When the distance from the center of the pile is $3d$, the ratio of the excess pore water pressure caused by pile driving in an untreated site to the effective overlying pressure was 1.44, and the overall level is greater than that of the cement mixing pile and well dewatering site and the surcharge preloading site, indicating that both engineering measures effectively suppress the generation of excess pore water pressure and reduce the impact of excess pore water pressure on the pile driving process.

In summary, dewatering and drainage boards can effectively reduce excess pore water pressure generated during pile driving. This reduction mitigates the soil-squeezing effect and minimizes the impact of excess pore water pressure on pile displacement and stress, thereby reducing the occurrence of pile floating and deflection.

Author Contributions: Conceptualization, Z.J.; methodology, Z.J.; software, H.W.; validation, S.H., Q.Z., and X.Z.; investigation, Z.J.; writing—original draft preparation, H.W.; writing—review and editing, S.H.; supervision, Z.J.; funding acquisition, Z.J. All authors have read and agreed to the published version of the manuscript.

Funding: The authors acknowledge funding from the Open Research Fund of State Key Laboratory of Geomechanics and Geotechnical Engineering, Institute of Rock and Soil Mechanics, Chinese Academy of Sciences (SKLGME022004), and the Hebei Natural Science Foundation (E2024402142).

Data Availability Statement: The original contributions presented in the study are included in the article; further inquiries can be directed to the corresponding authors.

Acknowledgments: Thanks to the Open Research Fund of State Key Laboratory of Geotechnical Mechanics and Geotechnical Engineering, Institute of Geotechnical Mechanics, Chinese Academy of Sciences Grant NO. SKLGME022004, and the experimental equipment support of Tianjin Guoda Measurement and Control Technology Co., Ltd.

Conflicts of Interest: The authors declare that research was conducted in the absence of any commercial or financial relationships that could be construed as potential conflicts of interest.

References

1. Zhang, X.; Shi, B.; Zhu, H.-H.; Zhang, C.-C.; Wang, X.; Sun, M.-Y. Performance monitoring of offshore PHC pipe pile using BOFDA-based distributed fiber optic sensing system. *Geomech. Eng.* **2021**, *24*, 337–348.
2. Zhang, Z.-M.; Yu, J.; Zhang, G.-X.; Wang, L.-Z. Contrastive experimental analysis of bearing behaviors of PHC pile and precast square piles. *Rock Soil Mech.* **2008**, *29*, 3059–3065.
3. Su, E.-W. PHC pile bearing capacity and application. *Adv. Mater. Res.* **2013**, *476–478*, 759–762. [[CrossRef](#)]
4. Xing, H.-F.; Zhao, H.-W.; Ye, G.-B.; Xu, C. Analysis of engineering characteristics of PHC pipe piles. *Rock Soil Mech.* **2009**, *31*, 36–39.
5. Jiao, Z.-B.; Wang, Z.-P.; Li, J.-L. Excavation problems induced by pile driving and their treatment. *Rock Soil Mech.* **2012**, *27*, 2246–2249.
6. Hwang, J.-H.; Liang, N.; Chen, C.-H. Ground response during pile driving. *J. Geotech. Geoenviron.* **2001**, *127*, 939–949. [[CrossRef](#)]
7. Kuo, Y.-S.; Chong, K.-J.; Tseng, Y.-H.; Hsu, H.-T. Excess pore water pressure response of soil inside the mini bucket embedded in saturated soil under seismic loading. *Soil Dyn. Earthq. Eng.* **2024**, *182*, 108751. [[CrossRef](#)]
8. Savvides, A.A.; Manolis, P. A computational study on the uncertainty quantification of failure of clays with a modified Cam-Clay yield criterion. *SN Appl. Sci.* **2021**, *3*, 659. [[CrossRef](#)]
9. Dou, J.-L.; Chen, J.-J.; Liao, C.-C. Method for estimating initial excess pore pressure during pile jacking into saturated fine-grained soil. *Comput. Geotech.* **2019**, *116*, 103203. [[CrossRef](#)]
10. Yao, X.-Q.; Hu, Z.-X. Estimating method for excess pore water pressure developed during pile driving. *Rock Soil Mech.* **1997**, *18*, 30–35.
11. Zhang, Y.; Wan, L.; Huang, Y.; Fu, J. Study on pore water pressure model of soft clay. *Adv. Mater. Res.* **2012**, *446–449*, 1510–1513. [[CrossRef](#)]
12. Osman, A.S.; Randolph, M.F. Analytical solution for the consolidation around a laterally loaded pile. *Int. J. Geomech.* **2012**, *12*, 199–208. [[CrossRef](#)]
13. Ganesalingam, D.; Read, W.; Nagaratnam, S. Consolidation behavior of a cylindrical soil layer subjected to nonuniform pore-water pressure distribution. *Int. J. Geomech.* **2013**, *13*, 665–671. [[CrossRef](#)]

14. Khanmohammadi, M.; Fakharian, K. Numerical modelling of pile installation and set-up effects on pile shaft capacity. *Int. J. Geotech. Eng.* **2019**, *13*, 484–498. [[CrossRef](#)]
15. Wang, Y.-H.; Liu, X.-Y.; Zhang, M.-Y.; Yang, S.-C.; Sang, S.-K. Field test of excess pore water pressure at pile-soil interface caused by PHC pipe pile penetration based on silicon piezoresistive sensor. *Sensors* **2020**, *20*, 2829. [[CrossRef](#)]
16. Ding, J.-W.; Wan, X.; Hong, Z.-S.; Wang, J.-H.; Mou, C. Excess pore water pressure induced by installation of precast piles in soft clay. *Int. J. Geomech.* **2021**, *21*. [[CrossRef](#)]
17. Ni, P.-P.; Mangalathu, S.; Mei, G.-X.; Zhao, Y.-L. Laboratory investigation of pore pressure dissipation in clay around permeable piles. *Can. Geotech. J.* **2017**, *55*, 1257–1267. [[CrossRef](#)]
18. Yang, Y.S.; Lei, J.B.; Deng, D.Z.; Zou, Y.Q. Laboratory Model Test and Analysis of Excess Pore Water Pressure Dissipation of Pile Driven by Tapered-Perforated Tubular Pipe Pile. *Earth. Environ. Sci.* **2021**, *62*, 042112. [[CrossRef](#)]
19. Hu, X.-Q.; Jiao, Z.-B.; Li, Y.-H. Distribution and dissipation laws of excess static pore water pressures induced by pile driving in saturated soft clay with driven plastic drainage plates. *Rock Soil Mech.* **2011**, *32*, 3733–3737.
20. Hu, X.-Q.; Zhao, X.-T.; Huang, H.-G.; Long, G.-T. Parameters analysis on construction control of precast piles in soft soil ground. *Adv. Mater. Res.* **2012**, *616–618*, 326–331. [[CrossRef](#)]
21. Fattah, Y.M.; Mustafa, S.F. Development of Excess Pore Water Pressure around Piles Excited by Pure Vertical Vibration. *Int. J. CIV Eng.* **2017**, *15*, 907–920. [[CrossRef](#)]
22. Fattah, Y.M.; Salman, A.F.; Al-Shakarchi, J.Y.; Raheem, A.M. Coupled pile-soil interaction analysis in undrained condition. *J. Cent. South Univ.* **2013**, *20*, 1376–1383. [[CrossRef](#)]
23. Tang, S.-D.; He, L.-S.; Fu, Z. Excess pore water pressure caused by an installing pile in soft foundation. *Rock Soil Mech.* **2002**, *23*, 725–729, 732.
24. Wang, H.-L.; Liu, Z.-K.; Guo, Q.J. Effect of pile driving on properties of soft clay foundation. *Chin. J. Rock. Mech. Eng.* **2003**, *22*, 2536–2540.
25. Li, F.-R.; Sun, H.-C.; Wang, Z.-Y. Mechanism Analysis and Experimental Study of Soil-Compacting by Silent Piling. *Adv. Mater. Res.* **2012**, *170–173*, 457–460. [[CrossRef](#)]
26. Ma, Z.-T.; Liu, H.-L.; Wang, Y.-P.; Zhu, J.-M. Field Test Research on Soil Compacting Effect of Cast-In Situ Concrete Pipe Pile. *Adv. Mat. Res.* **2012**, *446–449*, 1914–1917. [[CrossRef](#)]
27. Wang, Y.-X.; Sun, J. Influence of pile driving on properties of soils around pile and pore water pressure. *Chin. J. Rock Mech. Eng.* **2004**, *23*, 153–158.
28. Ozener, P.T.; Ozaydin, K.; Berilgen, M.M. Investigation of liquefaction and pore water pressure development in layered sands. *Bull. Earthq. Eng.* **2009**, *7*, 199–219. [[CrossRef](#)]
29. Zhang, H.; Zhang, J.-M.; Zhang, Z.; Zhang, M.-Y.; Cao, W. Variation behavior of pore-water pressure in warm frozen soil under load and its relation to deformation. *Acta Geotech.* **2020**, *15*, 603–614. [[CrossRef](#)]
30. Zhang, X.-L.; Zhu, D.-Z.; Xu, C.-S.; Du, X.-L. Research on p-y curves of soil-pile interaction in saturated sand foundation in weakened state. *Rock Soil Mech.* **2020**, *41*, 2252–2260.
31. Bai, B.; Liu, Z.-D. Growth and dissipation of pore water pressure in saturated soft clay under impact loading. *Rock Soil Mech.* **1998**, *19*, 33.
32. Dou, J.-Z.; Chen, J.-J.; Liao, C.-C.; Sun, M.; Han, L. Study on the correlation between soil consolidation and pile set-up considering pile installation effect. *J. Mar. Sci. Eng.* **2021**, *9*, 705. [[CrossRef](#)]
33. Bian, L.-M.; Xu, H.-B.; Xu, J.-P. Summary of research on the effect of driving pile. *J. Civ. Eng. Manag.* **2002**, *3*, 68–72.
34. Wang, W.-T.; Qiu, H.-J.; Zhan, H.-Q. Study on prediction and prevention for soil displacement caused by the statically pressed piles. *Chin. J. Geotech. Eng.* **2001**, *3*, 378–379.
35. Xie, Y.-J.; Wang, H.-Z.; Zhu, H.-H. Soil plugging effect of PHC pipe pile during driving into soft clay. *Rock Soil Mech.* **2009**, *30*, 1671–1675.
36. Zhu, Y.-W.; Cai, Y.-Q.; Xu, H. *ABAQUS and Geotechnical Engineering Analysis*; Tushu Publishing Limited: Hong Kong, China, 2005.
37. Huang, Q.-H.; Zou, Y.-H. Analysis of fast drained and consolidated mechanism of soft soil under excessive pore water pressure. *Adv. Mater. Res.* **2012**, *170–173*, 909–913. [[CrossRef](#)]
38. Sun, Y.-S.; Hong, H.; Jia, G.-F.; Zheng, X.-W. Pore water pressure observation technology. *Commun. Sci. Technol. HLJ* **2000**, *87*, 28–29.
39. Zhao, X.-S.; Sun, R.-M.; Yang, F.-L. Study on problem in Embedded installation of pore water pressure gauge. *Metal Mine* **2007**, *6*, 47–50.
40. Wei, L.-M.; He, Q.; Sun, Y.-N. Measurement and analysis of consolidation process for sand drain ground. *J. Cent. South Univ.* **2004**, *6*, 1019–1024.

Disclaimer/Publisher’s Note: The statements, opinions and data contained in all publications are solely those of the individual author(s) and contributor(s) and not of MDPI and/or the editor(s). MDPI and/or the editor(s) disclaim responsibility for any injury to people or property resulting from any ideas, methods, instructions or products referred to in the content.